

# Value of information in closed-loop reservoir management

E. G. D. Barros<sup>1</sup> · P. M. J. Van den Hof<sup>2</sup> · J. D. Jansen<sup>1</sup>

Received: 5 November 2014 / Accepted: 10 June 2015 / Published online: 4 August 2015  
© The Author(s) 2015. This article is published with open access at Springerlink.com

**Abstract** This paper proposes a new methodology to perform value of information (VOI) analysis within a closed-loop reservoir management (CLRM) framework. The workflow combines tools such as robust optimization and history matching in an environment of uncertainty characterization. The approach is illustrated with two simple examples: an analytical reservoir toy model based on decline curves and a water flooding problem in a two-dimensional five-spot reservoir. The results are compared with previous work on other measures of information valuation, and we show that our method is a more complete, although also more computationally intensive, approach to VOI analysis in a CLRM framework. We recommend it to be used as the reference for the development of more practical and less computationally demanding tools for VOI assessment in real fields.

**Keywords** Value of information · Value of clairvoyance · Decision making · Geological uncertainties · Closed-loop reservoir management · Model-based optimization · History matching · Well production data

## 1 Introduction

Over the past decades, numerical techniques for reservoir model-based optimization and history matching have developed rapidly, while it also has become possible to obtain increasingly detailed reservoir information by deploying different types of well-based sensors and field-wide sensing methods. Many of these technologies come at significant costs, and an assessment of the associated value of information (VOI) becomes therefore increasingly important (Kikani [11], ch. 3). In particular assessing the value of future measurements during the field development planning (FDP) phase of an oil field requires techniques to quantify the VOI under geological uncertainty. An additional complexity arises when it is attempted to quantify the VOI for closed-loop reservoir management (CLRM), i.e., under the assumption that frequent life-cycle optimization will be performed using frequently updated reservoir models. This paper describes a methodology to assess the VOI in such a CLRM context.

In Section 2, we introduce the most relevant concepts and review some previous work on information measures. Next, in Section 3, we present the proposed workflow for VOI analysis and thereafter, in Section 4, we illustrate it with some case studies in which results of the VOI calculations are analyzed and compared with other information measures.

---

✉ E. G. D. Barros  
e.barros@tudelft.nl

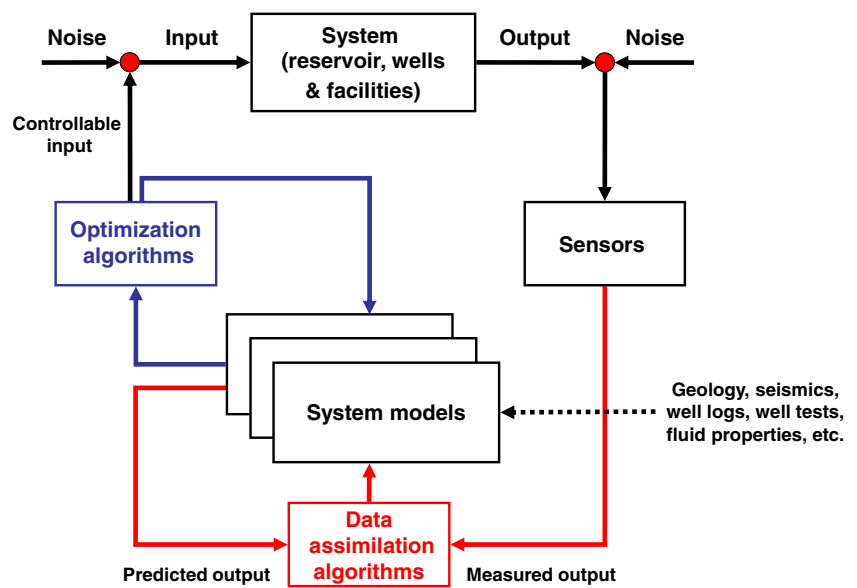
P. M. J. Van den Hof  
p.m.j.vandenhof@tue.nl

J. D. Jansen  
j.d.jansen@tudelft.nl

<sup>1</sup> Department of Geoscience and Engineering, Delft University of Technology, Delft, Netherlands

<sup>2</sup> Department of Electrical Engineering, Eindhoven University of Technology, Eindhoven, Netherlands

**Fig. 1** Closed-loop reservoir management as a combination of life-cycle optimization and data assimilation



Finally, in Section 5, we address the computational aspects of applying this workflow to real field cases, and we suggest a direction for further research

## 2 Background

### 2.1 Closed-loop reservoir management

Closed-loop reservoir management (CLRM) is a combination of frequent life-cycle production optimization and data assimilation (also known as computer-assisted history matching) (see Fig. 1). Life-cycle optimization aims at maximizing a financial measure, typically net present value (NPV), over the producing life of the reservoir by optimizing the production strategy. This may involve well location optimization, or, in a more restricted setting, optimization of well rates and pressures for a given configuration of wells, on the basis of one or more numerical reservoir models. Data assimilation involves modifying the parameters of one or more reservoir models, or the underlying geological models, with the aim to improve their predictive capacity, using measured data from a potentially wide variety of sources such as production data or time-lapse seismic. For further information on CLRM see, e.g., Jansen et al. [8–10], Naevdal et al. [16], Sarma et al. [19], Chen et al. [4], and Wang et al. [22].

### 2.2 Robust optimization

An efficient model-based optimization algorithm is one of the required elements for CLRM. Because of the inherent uncertainty in the geological characterization of the subsurface, a non-deterministic approach is necessary. Robust life-cycle optimization uses one or more ensembles of

geological realizations (reservoir models) to account for uncertainties and to determine the production strategy that maximizes a given objective function over the ensemble (see, e.g., Yeten et al. [21] or Van Essen et al. [20]). Figure 2 schematically represents robust optimization over an ensemble of  $N$  realizations  $\{\mathbf{m}_1, \mathbf{m}_2, \dots, \mathbf{m}_N\}$ , where  $\mathbf{m}$  is a vector of uncertain model parameters (e.g., grid block permeabilities or fault multipliers). The objective function  $J_{NPV}$  is defined as

$$J_{NPV} = \frac{1}{N} \sum_{i=1}^N J_i, \quad (1)$$

i.e., as the ensemble mean (expected value) of the objective function values  $J_i$  of the individual realizations. The objective function  $J_i$  for a single realization  $i$  is defined as

$$J_i = \int_{t=0}^T \frac{q_o(t, \mathbf{m}_i) r_o - q_{wp}(t, \mathbf{m}_i) r_{wp} - q_{wi}(t, \mathbf{m}_i) r_{wi}}{(1+b)^{t/\tau}} dt, \quad (2)$$

where  $t$  is time,  $T$  is the producing life of the reservoir,  $q_o$  is the oil production rate,  $q_{wp}$  is the water production rate,

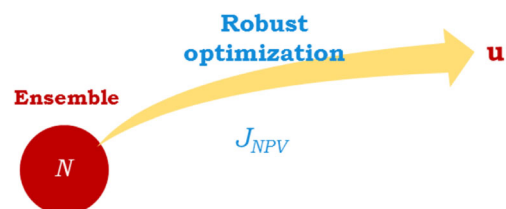


**Fig. 2** Robust optimization: optimizing the objective function of an ensemble of  $N$  realizations resulting in a single control vector  $\mathbf{u}$

$q_{wi}$  is the water injection rate,  $r_o$  is the price of oil produced,  $r_{wp}$  is the cost of water produced,  $r_{wi}$  is the cost of water injected,  $b$  is the discount factor expressed as a fraction per year, and  $\tau$  is the reference time for discounting (typically 1 year). The outcome of the optimization procedure is a vector  $\mathbf{u}$  containing the settings of the control variables over the producing life of the reservoir. Note that, although the optimization is based on  $N$  models, only a single strategy  $\mathbf{u}$  is obtained. Typical elements of  $\mathbf{u}$  are monthly or quarterly settings of well head pressures, water injection rates, valve openings, etc.

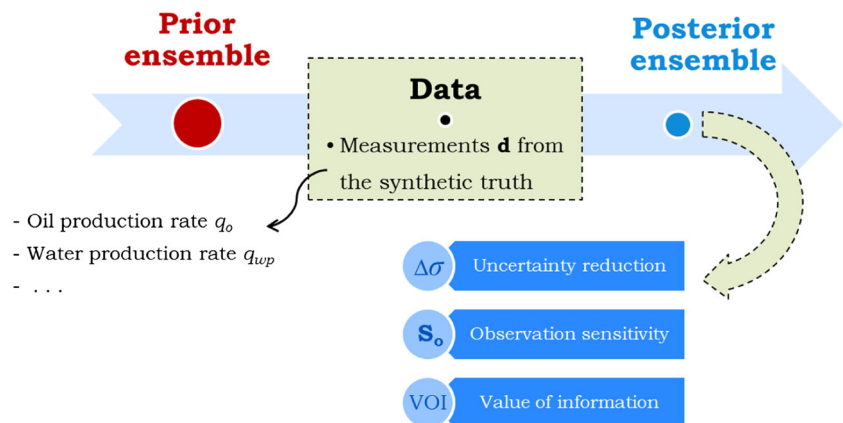
### 2.3 Data assimilation

Efficient data assimilation algorithms are also an essential element of CLRM. Many methods for reservoir-focused data assimilation have been developed over the past years, and we refer to Oliver et al. [17], Evensen [5], Aanonsen et al. [1], and Oliver and Chen [18] for overviews. An essential component of data assimilation is accounting for uncertainties, and it is generally accepted that this is best done in a Bayesian framework:

$$p(\mathbf{m}|\mathbf{d}) = \frac{p(\mathbf{d}|\mathbf{m})p(\mathbf{m})}{p(\mathbf{d})}, \tag{3}$$

where  $p$  indicates the probability density and  $\mathbf{d}$  is a vector of measured data (e.g., oil and water flow rates or saturation estimates from time-lapse seismic). In Eq. 3, the terms  $p(\mathbf{m})$  and  $p(\mathbf{m}|\mathbf{d})$  represent the *prior* and *posterior* probabilities of the model parameters  $\mathbf{m}$ , which are, in our setting, represented by prior and posterior ensembles, respectively. The underlying assumption in data assimilation is that a reduced uncertainty in the model parameters leads to an improved predictive capacity of the models, which, in turn, leads to improved decisions. In our CLRM setting, decisions take the form of control vectors  $\mathbf{u}$ , aimed at maximizing the objective function  $J$ .

**Fig. 3** Data assimilation and information valuation



### 2.4 Information valuation

Previous work on information valuation in reservoir engineering focused on analyzing how additional information impacts the model predictions. One way of valuing information is proposed by Krymskaya et al. [12]. They use the concept of *observation impact*, which was first introduced in atmospheric modelling. Starting from a Bayesian framework, they derive an *observation sensitivity matrix*  $\mathbf{S}$  which contains self and cross-sensitivities (diagonal and off-diagonal elements of the matrix, respectively). The self-sensitivities, which quantify how much the observation of measured data impacts the prediction of these same data by a history-matched model, provide a measure of the information content in the data. Their joint influence can be expressed with a global average influence index defined as

$$I_{GAI} = \frac{tr(\mathbf{S})}{N_{obs}}, \quad 0 \leq I_{GAI} \leq 1, \tag{4}$$

where  $N_{obs}$  is the number of observations (i.e., the number of diagonal elements in  $\mathbf{S}$ ).

Another approach is taken by Le and Reynolds [13, 14] who address the usefulness of information in terms of the reduction in uncertainty of a variable of interest (e.g., NPV). They introduce a method to estimate, in a computationally feasible way, how much the assimilation of an observation contributes to reducing the spread in the predictions of the variable of interest, expressed as the difference between  $P_{10}$  and  $P_{90}$  percentiles, i.e., between the 10 and 90 % cumulative probability density levels.

Both approaches are based on data assimilation, and Fig. 3 schematically represents how measured data are used to update a prior ensemble of reservoir models, resulting in a posterior ensemble which forms the basis to compute various measures of information valuation. In Fig. 3, the measurements are obtained in the form of synthetic data generated by a *synthetic truth*. This preempts our proposed method of information valuation in which we will use an ensemble of models in the FDP stage, of which each



random variable. One of the underlying assumptions of our proposed workflow is that the truth is a realization from the same probability distribution function as used to create the realizations of the ensemble. Hence, the methodology only allows to quantify the VOI under uncertainty in the form of *known unknowns*. Obviously, specifying uncertainty in the form of *unknown unknowns* is impossible, which therefore is a fundamental shortcoming in any VOI analysis. (I.e., we may think that we know the complete reservoir description (as captured in the prior ensemble), but we may have missed “unmodelled” features such as an unexpected aquifer or a sub-seismic fault.)

Because any of the  $N$  models in the initial ensemble could be the truth, the procedure has to be repeated  $N$  times, consecutively letting each one of the initial models act as the synthetic truth. This allows us to quantify the *expected VOI* over the entire ensemble:

$$VOI = \bar{J}_{NPV} = \frac{1}{N} \sum_{i=1}^N \left( J_{NPV, post}^i - J_{NPV, prior}^i \right). \quad (5)$$

We note that this repetition is similar to the use of multiple plausible truth cases in Le and Reynolds [13, 14]. We also note that in the literature on VOI, most of the times the term VOI is used to refer to the expected VOI. The flowchart in Fig. 5 shows the complete procedure. A further remark concerns the size of the initial ensemble ( $N$  members) and those of the prior ensembles ( $N-1$  members). This choice results from our approach to start by generating  $N$  ensembles of  $N$  members each and subsequently selecting one member from each of the  $N$  ensembles to be part of the initial ensemble, such that the  $N$  ensembles with the remaining  $N-1$  members form the prior ensembles. However, other choices would be equally possible. Finally, we note that, to be absolutely rigorous, we would have to repeat the whole workflow several times with different realizations of the noise in the observation vectors. However, we argue that by far the largest contribution to uncertainty originates from the geology, as captured in the various ensembles of geological realizations. In comparison, the effect of measurement noise is small and sufficiently captured by using a new noise realization for each synthetic measurement.

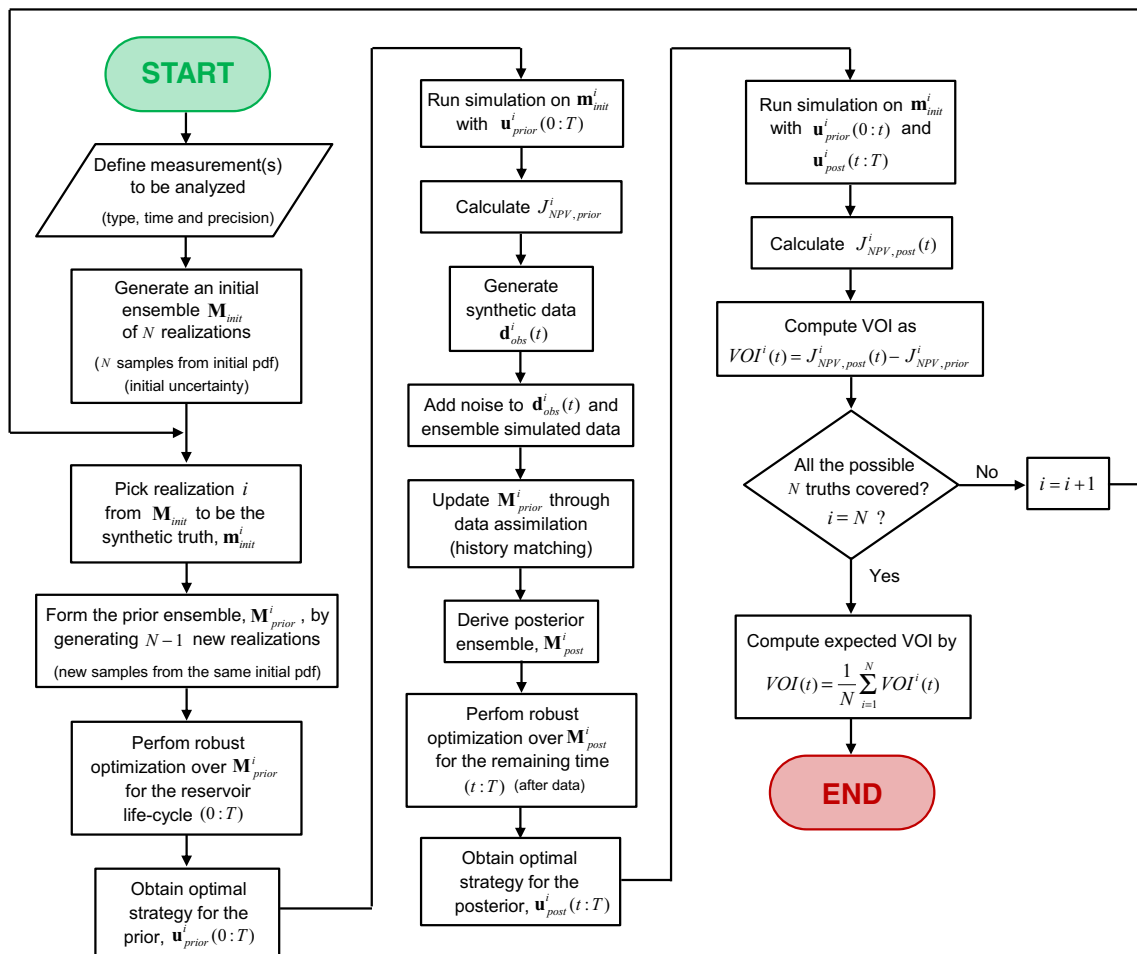


Fig. 5 Complete workflow to compute the expected VOI

The workflow can be adapted to compute the expected *value of clairvoyance* (VOC), which simply means that at some time in the reservoir life, we suddenly know the truth so we can perform life-cycle production optimization on the true reservoir model. The estimated expectation of VOC is then computed from Eq. 5 where each posterior NPV is obtained while applying the optimal controls determined for the associated synthetic true model. Such a clairvoyance implies the availability of completely informative data without observation errors, and the expected VOC therefore forms a theoretical upper bound (i.e., a “technical limit”) to the expected VOI. Moreover, because this modified workflow does not require data assimilation, and, after the truth has been revealed, only requires optimization of a single (true) model, it is computationally significantly less demanding.

## 4 Examples

### 4.1 Toy model

As a first step to test the proposed concept, we used a very simple model with only a few parameters, based on reservoir decline curves. It describes oil and water flow rates  $q_o$  and  $q_w$  as a function of time  $t$  and a scalar control variable  $u$  according to the following expressions:

$$q_o(u, t) = (q_{o,\text{ini}} + c_1 u) \exp\left(-\frac{t}{a + \frac{1}{c_2} u}\right), \quad (6)$$

$$q_w(u, t) = H\left[t_{\text{bt}}\left(1 - \frac{1}{c_3} u\right)\right] (q_{w,\infty} + u) \left[1 - \exp\left(-\frac{t - t_{\text{bt}}\left(1 - \frac{1}{c_3} u\right)}{c_4 a - \frac{1}{c_5} u}\right)\right], \quad (7)$$

where  $q_{o,\text{ini}}$  is the initial production rate,  $t_{\text{bt}}$  is the water breakthrough time, and  $q_{w,\infty}$  is the asymptotic water production rate, all for a situation without control, i.e., for  $u = 0$ . The oil production follows an exponential decline, and

the water production builds up exponentially from a breakthrough time modelled by a Heaviside step function  $H$ . The variables have dimensions as listed in Table 1, where  $L$ ,  $M$ , and  $t$  indicate length, monetary value, and time, respectively. Some of the parameters are constants, while four uncertain parameters are normally distributed with values indicated in Table 1. The scalar control variable  $u$  somehow mimics a water injection rate to the reservoir; higher values of  $u$  slow down the decline of oil production but accelerate water breakthrough and increase water production, as shown in Fig. 6. Given the prices and costs associated with oil and water production, there is room for optimization to determine the value of  $u$  that maximizes the economics of the reservoir over a fixed producing life-time. To allow for regular updating of the control strategy over the producing life of the reservoir, the scalar  $u$  can be replaced by a vector  $\mathbf{u} = [u_1 \ u_2 \ \dots \ u_M]^T$ , where  $M$  is the number of control intervals.

The question to be answered here was as follows: given an initial ensemble of models describing the geological uncertainties and an initial optimized control vector  $\mathbf{u}$ , what is the value of a production test in the form of a measurements  $\mathbf{d} = [q_o(t_{\text{data}}) \ q_w(t_{\text{data}})]^T$  of oil and water production rates at a given time  $t_{\text{data}}$ , for different measurement errors and observation times? The VOI assessment procedure described in the previous section was applied, and repeated for different observation times,  $t_{\text{data}} = \{1, 2, \dots, 80\}$ . We used a random measurement error with a standard deviation  $\sigma_{\text{data}}$  equal to 5 % of the measured value, an ensemble of  $N = 100$  model realizations and  $M = 8$  control time steps. Ensemble optimization (EnOpt) and ensemble Kalman filtering (EnKF) were used to perform the robust optimization and the data assimilation respectively. (We used the robust EnOpt implementation of Fonseca et al. [6] which is a modified form of the original formulation proposed by Chen et al. [4].) For general information on EnKF, see, e.g., Evensen [5] or Aanonsen et al. [1]; we used a straightforward implementation without localization or inflation.) The VOI, the VOC, the observation impact  $I_{\text{GAI}}$ , and the uncertainty reduction  $\Delta\sigma_{\text{NPV}}$  were computed for each of the 80 observation times. The average NPV for

**Table 1** Parameter values for toy model

Variables		Constant parameters		Uncertain parameters	
$q_o$	$[L^3 t^{-1}]$	$c_1 = 0.1$	$[-]$	$q_{o,\text{ini}} \sim N(100, 8)$	$[L^3 t^{-1}]$
$q_w$	$[L^3 t^{-1}]$	$c_2 = 4$	$[L^3 t^{-2}]$	$a \sim N(30.5, 3.67)$	$[t]$
$t \in [0, 80]$	$[t]$	$c_3 = 150$	$[L^3 t^{-1}]$	$q_{w,\infty} \sim N(132, 6)$	$[L^3 t^{-1}]$
$u \in [10, 50]$	$[L^3 t^{-1}]$	$c_4 = 2$	$[-]$	$t_{\text{bt}} \sim N(32, 6)$	$[t]$
		$c_5 = 1.33$	$[L^3 t^{-2}]$		
		$r_o = 70$	$M L^{-3}$		
		$r_w = 10$	$M L^{-3}$		
		$b = 0.10$	$[-]$		



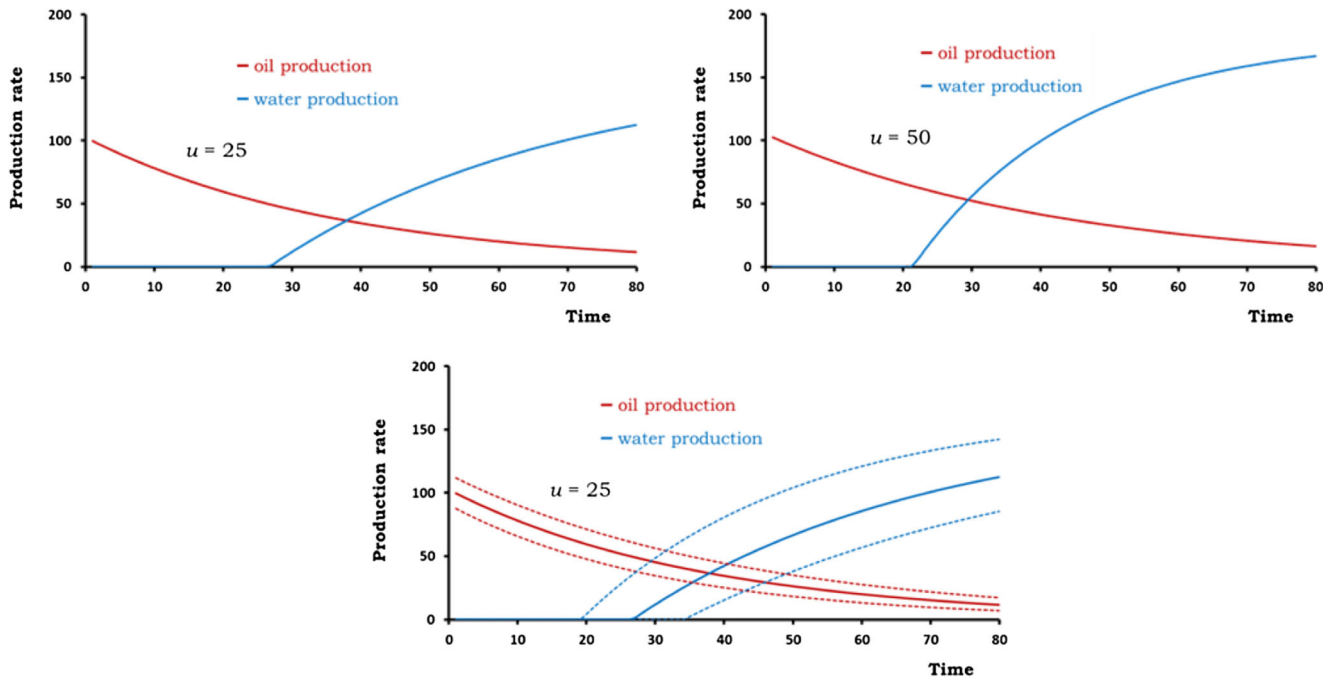


**Fig. 6** Toy model behavior: oil and water production for two fixed values of the control variable  $u$  (*top*); representation of uncertainty in the form of  $P_{10}$  and  $P_{90}$  percentiles (*bottom*)

the initial ensemble is \$108,900 when using base line control (i.e., the average of the upper (50) and lower bounds (10),  $\mathbf{u}_{ini} = \{30, 30, \dots, 30\}$ ) and \$114,300 when using robust optimization over the prior (i.e., without additional information). The initial uncertainty is  $\sigma_{NPV,ini} = \$11,960$ , computed as the average of the standard deviations in the NPV of the different prior ensembles. We repeated the optimization by starting from a more aggressive initial strategy where the values of  $\mathbf{u}_{ini}$  were at their bounds, which gave near-identical results.

The expected VOC as a function of observation time  $t_{data}$  is depicted in Fig. 7 (top left), where we expressed the monetary value, arbitrarily, in \$. The dashed line represents the expected VOC, i.e., the ensemble mean. The dark solid line and the two lighter solid lines represent the  $P_{50}$  and  $P_{10}/P_{90}$  percentiles, respectively. Here,  $P_x$  is defined as the probability that  $x\%$  of the outcomes exceeds this value. The expected VOC is the value one could obtain if the truth could be revealed and all the uncertainty could be eliminated at no costs at time  $t_{data}$ . Of course, these results depend on the operation schedule (i.e., the number of control time steps) and on the initial ensemble of realizations that characterize the uncertainty. As can be seen, the VOC exhibits a stepwise decrease over time, with the steps coinciding with the eight control time steps. This stepwise behavior occurs because knowing the truth only affects the way one operates the reservoir from the moment of clairvoyance and because the production strategy can only be updated at the defined control time steps. The sooner clairvoyance is available, the

more control time steps can be tuned to re-optimize the production strategy based on the truth, and, therefore, the more value is obtained. Thus, this plot demonstrates the importance of timing when collecting additional information to make decisions. Even clairvoyance can be completely useless ( $VOC = 0$ ) when it is obtained too late (in this case after  $t_{data} = 40$ ).

The percentiles of the VOC distribution in Fig. 7 (top left) illustrate that the VOC is itself a random variable, because, despite knowing that the truth has been revealed, it is not possible to know which of the model realizations is this truth; all members of the initial ensemble are potentially true in the design phase. Hence, the VOC for a particular case may be higher or lower than the expected VOC.

In a similar fashion, Fig. 7 (top right, bottom left, and bottom right) displays the VOI, the uncertainty reduction in NPV, and the observation impact as a function of observation time  $t_{data}$ . In Fig. 7 (bottom right), the peak in the observation impact indicates that production data is most informative around  $t_{data} = 30$ ; in Fig. 7 (bottom right), the uncertainty reduction follows the same trend; and, in Fig. 7 (top left), the VOI also increases at the same time. This suggests that, in this example, measurements with a higher observation impact also result in a larger uncertainty reduction in NPV and a higher VOI. However, whereas the observation impact and the uncertainty reduction both peak around  $t_{data} = 30$  and gently decrease afterwards, the VOI exhibits a more abrupt decrease, similar to what is observed for the VOC. This indicates that the VOI depends not only

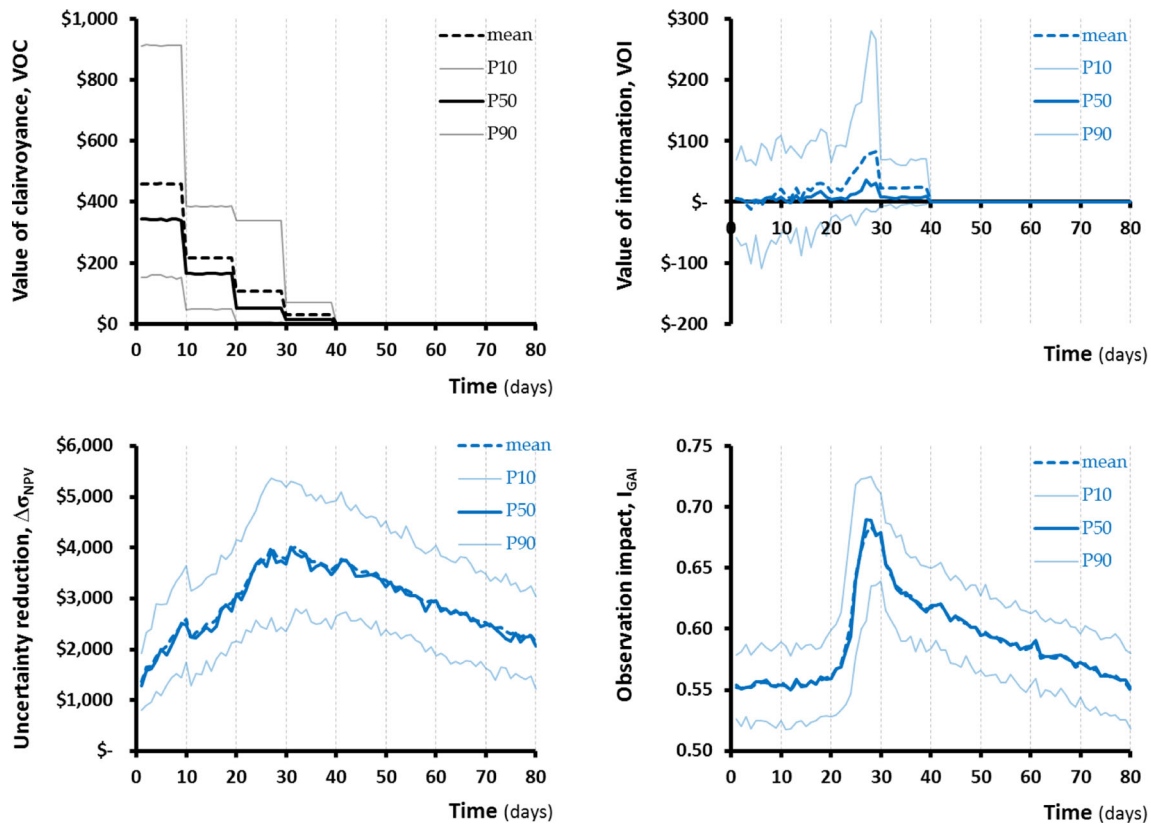


**Fig. 7** Results for the VOI analysis in the toy model: VOC (*top left*); VOI (*top right*); it should be: uncertainty reduction (*bottom left*) and observation impact (*bottom right*)

on the information content of the observations but also on their timing, just as was discussed for the VOC. Moreover, these results illustrate that the proposed workflow allows to take both information content and timing into account and, therefore, results in a more complete VOI assessment.

Figure 8 (left) shows the same results, but focusing on the expected (or mean) values of VOC (black) and VOI (blue). This plot clearly illustrates that the expected VOC is always an upper bound to the expected VOI. Indeed, production data, no matter how accurate, can never reveal all

uncertainties. After water breakthrough, production data is more informative and it is more likely that the uncertainties influencing the optimization of the production strategy be revealed; thus, information more closely approaches clairvoyance. Figure 8 (right) illustrates this in a different way by displaying the chance of knowing (COK), defined as the ratio  $VOI/VOC$  [2].

The different information measures suggest in this case that the most valuable measurements are the ones around  $t_{data} = 30$ . We conclude that a decision maker analyzing

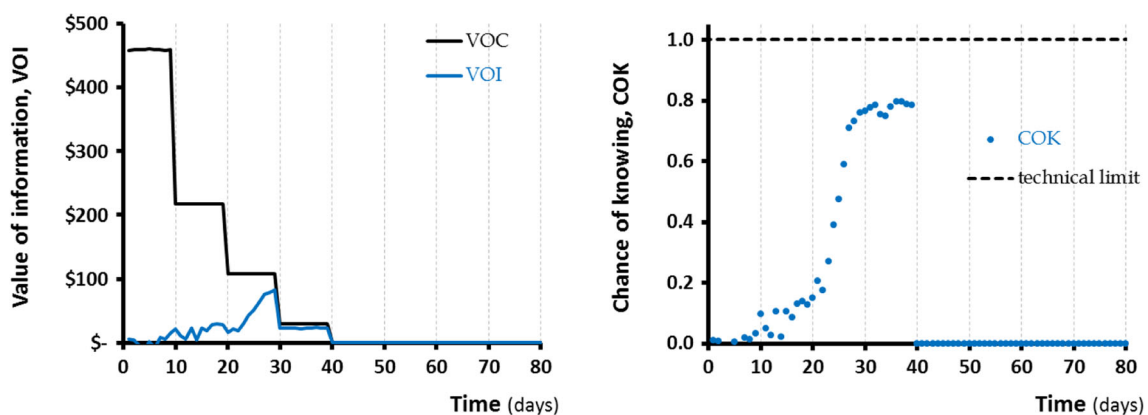


**Fig. 8** Results for the toy model: the expected VOI is upper-bounded by expected VOC (*left*); the ratio of VOI and VOC results in the COK (*right*)



when to obtain a production test to optimally operate this reservoir should take a measurement around this time and should be willing to pay at most approximately \$80—and not \$4,000 as the uncertainty reduction analysis would suggest. Note that the model we used in this example is very simple. The optimal strategies for the different realizations are quite similar, which means that the robust strategy (the one that maximizes the mean NPV of the ensemble) is already quite good for all the realizations. For that reason, in this case, the additional information does not lead to a significant improvement in the production strategy.

### 4.2 2D five-spot model

As a next step, we applied the proposed VOI workflow to a simple reservoir simulation model representing a two-dimensional (2D) inverted five-spot water flooding configuration (see Fig. 9). In a  $21 \times 21$  grid ( $700 \times 700$  m), with heterogeneous permeability and porosity fields, the model simulates the displacement of oil to the producers in the corners by the water injected in the center. Table 2 lists the values of the physical parameters of the reservoir model. We used 50 ensembles of  $N = 50$  realizations of the porosity and permeability fields, conditioned to hard data in the wells, to model the geological uncertainties. The simulations were used to determine the set of well controls (bottom hole pressures) that maximizes the NPV. The economic parameters considered in this example are also indicated in Table 2. The optimization was run for a 1,500-day time horizon with well controls updated every 150 days, i.e.,  $M = 10$ , and, with five wells,  $\mathbf{u}$  has 50 elements. We applied bound constraints to the optimization variables ( $200 \text{ bar} \leq p_{\text{prod}} \leq 300 \text{ bar}$  and  $300 \text{ bar} \leq p_{\text{inj}} \leq 500 \text{ bar}$ ). The initial control values were chosen as the average of the upper and lower bounds. The whole exercise was performed in the open-source reservoir simulator MRST Lie et al. [15], by modifying the adjoint-based optimization module to allow for robust optimization and combining it with the EnKF

**Table 2** Parameter values for 2D five-spot model

Rock-fluid parameters		Initial conditions	
$\rho_o = 800$	kg/m <sup>3</sup>	$p_0 = 300$	bar
$\rho_w = 1,000$	kg/m <sup>3</sup>	$S_{oi} = 0.8$	[-]
$\mu_o = 0.5$	cP	$S_{wi} = 0.2$	[-]
$\mu_w = 1$	cP		
$n_o = 2$	[-]	Economic parameters	
$S_{or} = 0.2$	[-]	$r_o = 80$	\$/bbl
$k_{ro,or} = 0.9$	[-]	$r_{wp} = 5$	\$/bbl
$n_w = 2$	[-]	$r_{wi} = 5$	\$/bbl
$S_{wc} = 0.2$	[-]	$b = 0.15$	[-]
$k_{rw,wc} = 0.6$	[-]		

module to create a CLRM environment for VOI analysis. The average NPV for the initial ensemble is \$53.5 million when using base line control (i.e., the average of the upper and lower bounds on the bottom hole pressures: 400 bar in the injector and 250 bar in the producers) and \$55.7 million when using robust optimization over the prior (i.e., without additional information). Just like for the toy model example, the workflow was repeated for different observation times,  $t_{\text{data}} = \{150, 300, \dots, 1350\}$  days. For this 2D model, we assessed the VOI of the production data (total flow rates and water-cuts) with absolute measurement errors ( $\epsilon_{\text{flux}} = 5 \text{ m}^3/\text{day}$  and  $\epsilon_{\text{wct}} = 0.1$ ). The VOI, the VOC, the observation impact  $I_{\text{GAI}}$ , and the uncertainty reduction  $\Delta\sigma_{\text{NPV}}$  were computed for each of the nine observation times.

Figure 10 depicts the results of the analysis for production data. Again, dashed lines correspond to expected values and solid lines to percentiles quantifying the uncertainty of the information measures. The markers correspond to the observation times at which the analysis was carried out. In Fig. 10 (top left), we note that, like for the toy model example, clairvoyance loses value with observation time, following the previously described stepwise behavior. In

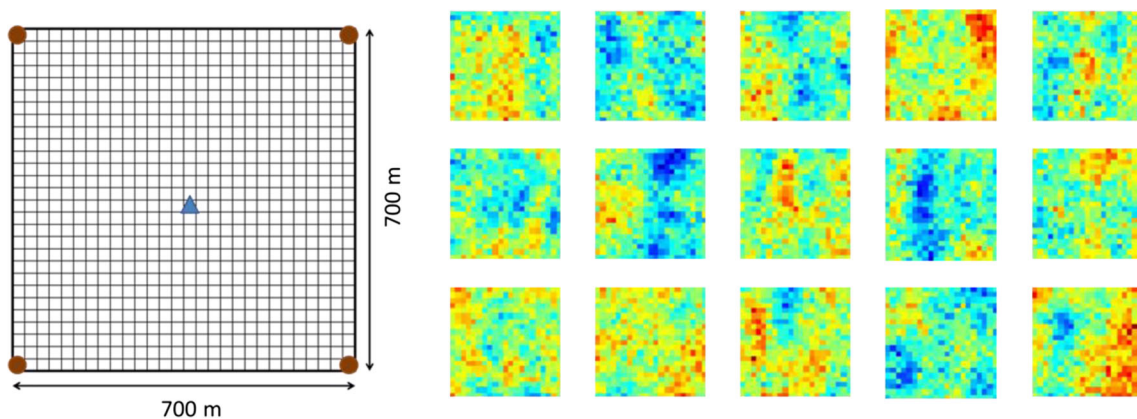


**Fig. 9** 2D five-spot model (left); 15 randomly chosen realizations of the uncertain permeability field (right)

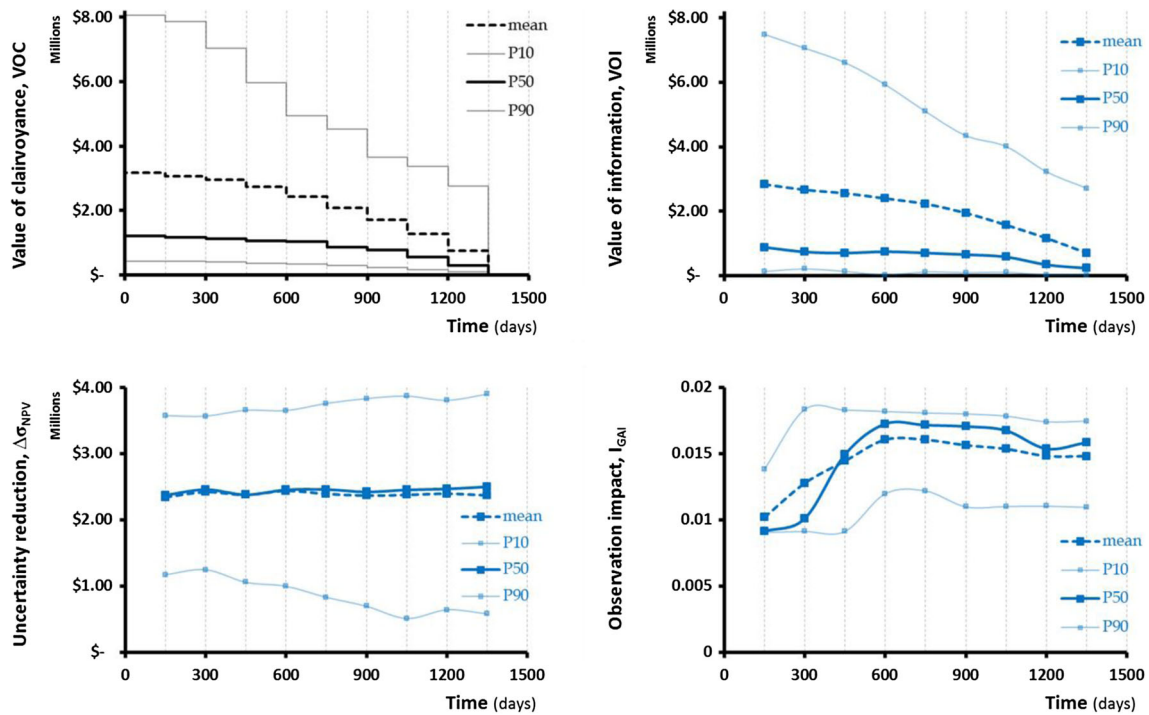


**Fig. 10** Results for the VOI analysis of production data in the 2D model: VOC (*top left*); VOI (*top right*); uncertainty reduction (*bottom left*) and observation impact (*bottom right*)

addition, by observing the percentiles, we realize that, in this case, the VOC has a non-symmetric probability distribution. The high values of P10 indicate that, for some realizations of the truth, knowing the truth can be considerably more valuable than indicated by the expected VOC; however, the P50 values, which are always below those of the expected VOC, indicate what is more likely to occur. The same holds for the VOI, as can be observed in Fig. 10 (top right). The observation that provides the best VOI is the one at  $t_{data} = 150$  days. Note that in our example, the earliest observation seems to be the most valuable one, but that this may be case-specific.

Figure 10 (bottom right) shows that the information content of the production data increases when water breaks

through in the producers but gently decreases thereafter. The observation impact achieves its maximum at  $t_{data} = 600$  days; this is the time when, on average, most of the realizations have already experienced first water breakthrough. Figure 10 (bottom left) displays the uncertainty reduction in NPV where the initial uncertainty is  $\sigma_{NPV,ini} = \$4.1$  million.

Figure 11 (left) depicts the expected values of VOI (blue dots) and VOC (black line). The plot confirms that clairvoyance can be considered the technical limit for any information gathering strategy and that the expected VOC forms an upper-bound to the expected VOI. We also note that the expected VOI comes closer to the expected VOC with time. Indeed, as water breakthrough is observed in more

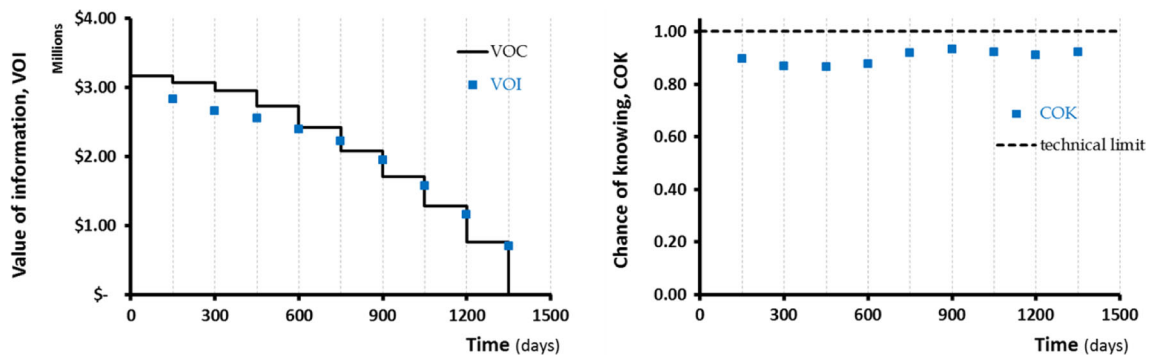


**Fig. 11** Results for the 2D model: the expected VOI is upper-bounded by expected VOC (*left*); the COK (*right*) is less informative than for the toy model (c.f. Fig. 8)

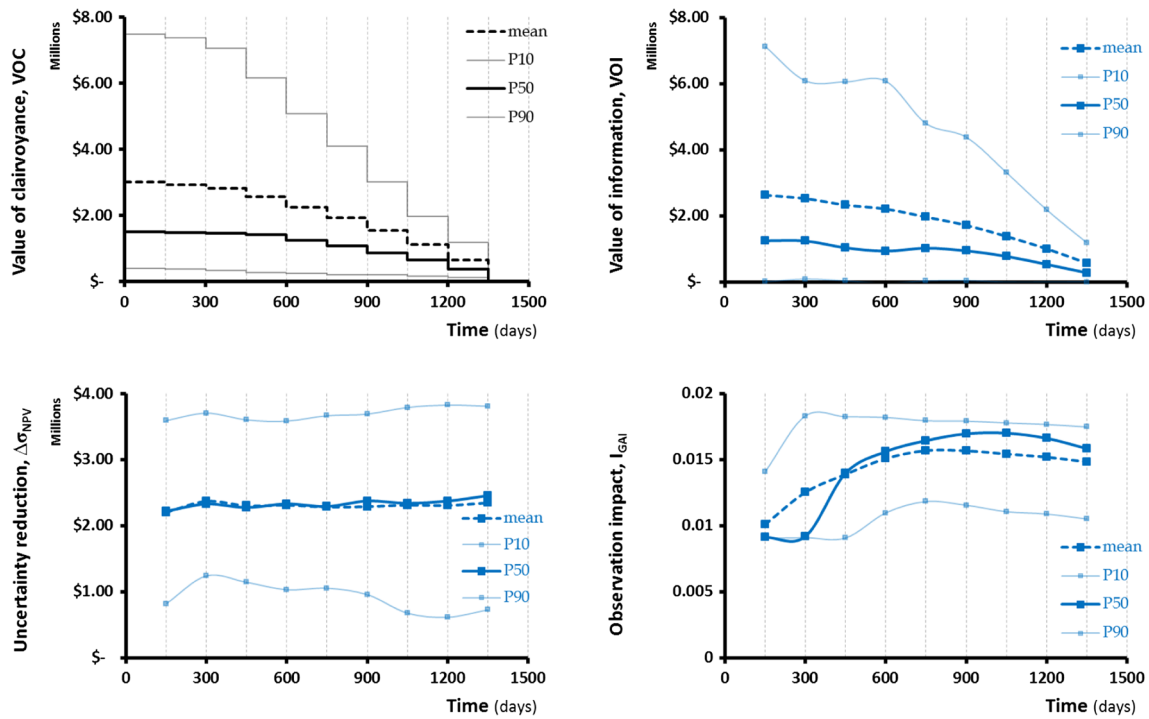


**Fig. 12** Results for the VOI analysis of production data in the 2D model using an accelerated procedure; VOC (*top left*); VOI (*top right*); uncertainty reduction (*bottom left*) and observation impact

(*bottom right*). The results are nearly identical to those of Fig. 10 although the uncertainty in the various measures is somewhat underestimated

producers, the production data of this five-spot pattern become more effective in revealing the main features of the true permeability and porosity fields. Figure 11 (right) displays the COK with time. Although the VOI clearly approaches the VOC, their ratio does not change substantially with time, unlike what was observed for the toy model example.

In contrast to the toy model case, for this example, the different information measures indicate different times for the most valuable measurements. This shows that taking into account the update of the optimal production strategy can influence the conclusions drawn by this kind of analysis. Using the proposed workflow as the reference for VOI

assessment, for this case, we recommend the production data to be collected at  $t_{data} = 150$  days, and we estimate this additional information to be worth \$2.8 million.

### 4.3 Accelerated procedure

We observed that there seems to be an opportunity to reduce the number of simulations required in the proposed workflow by using the complete initial ensemble to perform a single prior robust optimization (rather than performing the robust optimization  $N$  times for  $N$  priors). For instance, in our 2D example, we could reduce the number of prior robust optimizations from 50 to 1, which represents a

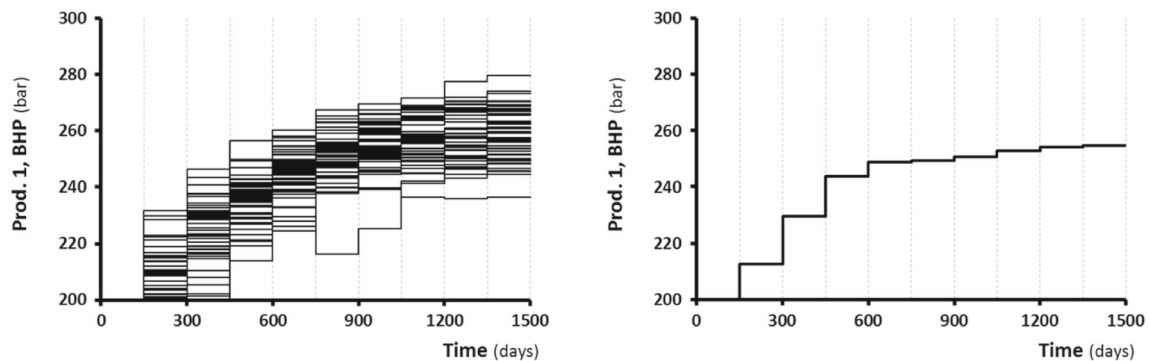


**Fig. 13** Optimal well controls (BHP) at producer 1 for the 50 different prior ensembles in the 2D model example; rigorous procedure (*left*); accelerated procedure (*right*). Similar differences were observed for the other wells in this example

significant reduction of the computational costs of the VOI assessment procedure: approximately 420,000 simulations for the original formulation and 215,000 for the modified formulation to compute the VOI for one observation time, and approximately 2,100,000 simulations for the original formulation and 1,895,000 simulations for the modified formulation to compute all the VOI values depicted in Figs. 10 and 11 (9 observation times). Figure 12 depicts the results for the VOI analysis of production data in the 2D model using the accelerated procedure. They are nearly identical to those of Fig. 10, which were obtained using the rigorous procedure, although the uncertainty in the various measures is somewhat under-estimated as can be seen from the difference between  $P_{10}$  and  $P_{90}$  values, especially at later times. This reduction in uncertainty results from the use of a single control strategy (based on a single prior robust optimization) instead of a set of different control strategies as obtained in the rigorous procedure (see Fig. 13). Note that the use of a single ensemble in the accelerated procedure only concerns the computation of the prior control strategy. The remainder of the procedure (columns 2 and 3 in Fig. 5) is still performed using  $N$  different ensembles.

## 5 Discussion and conclusion

We proposed a new workflow for VOI assessment in CLRM. The method uses elements available in the CLRM framework, such as history matching and robust optimization. First, we identified the opportunity to combine these elements with concepts of information value theory to create a VOI analysis instrument. We then designed a generic procedure that can, in theory, be simply implemented in a variety of applications, including our optimal reservoir management problem. Next, the workflow was illustrated with two examples and the results were compared with previous measures for information valuation. Because we take into account that the production strategy is updated after new information has been assimilated in the models, we believe that our proposed method is more complete than previous work to estimate the VOI in a reservoir engineering context.

The main drawback of our proposed VOI workflow is its computational costs; it involves the repeated application of robust optimization and data assimilation, which requires a very large number of reservoir simulations. Depending on the types of optimization and assimilation methods used (e.g., adjoint-based, ensemble-based, or gradient-free), there may be large differences in the computational requirements, but even in case of using the most efficient (i.e., adjoint-based) algorithms, the computational load of the workflow will be huge. For instance, for the toy model example with ensembles of 100 realizations, we ran more than 50 million forward simulations (8,100 robust

optimizations with EnOpt) in order to obtain one of the 80 values of VOI displayed in Fig. 7 (top right). Hence, if the method is to be applied to real-field cases, some serious improvements regarding the number of simulations required are necessary. In this paper, we showed a first step in this direction by suggesting a way to reduce the number of robust optimizations necessary. However, more has to be done. One potential method could be to use clustering techniques to select a few representative realizations rather than a full ensemble. Furthermore, reduced-order modelling techniques to generate surrogate models could facilitate the application of our workflow to larger reservoir models by reducing the number of full reservoir simulations. Despite its computational cost, we conclude that our approach constitutes a rigorous VOI assessment for CLRM. For this reason, we recommend that it be used as the reference for the development of more practical and less computationally demanding tools to be applied in real-field cases.

**Open Access** This article is distributed under the terms of the Creative Commons Attribution 4.0 International License (<http://creativecommons.org/licenses/by/4.0/>), which permits unrestricted use, distribution, and reproduction in any medium, provided you give appropriate credit to the original author(s) and the source, provide a link to the Creative Commons license, and indicate if changes were made.

**Acknowledgments** This research was carried out within the context of the ISAPP Knowledge Centre. ISAPP (Integrated Systems Approach to Petroleum Production) is a joint project of TNO, Delft University of Technology, ENI, Statoil and Petrobras. The EnKF module for MRST was developed by Olwijn Leeuwenburgh (TNO) and can be obtained from <http://www.isapp2.com/data-sharepoint/enkf-module-for-mrst>. We acknowledge the comments of the anonymous reviewers which helped to substantially improve the manuscript.

## References

1. Aanonsen, S.I., Naevdal, G., Oliver, D.S., Reynolds, A.C., Valles, B.: The ensemble Kalman filter in reservoir engineering – a review. *SPE J.* **14**(3), 393–412 (2009)
2. Bhattacharjya, D., Eidsvik, J., Mukerji, T.: The value of information in spatial decision making. *Math. Geosci.* **42**(2), 141–163 (2010)
3. Bratvold, R.B., Bickel, E.J., Lohne, H.P.: Value of information: the past, present, and future. *SPE Reserv. Eval. Eng.* **12**(4), 630–638 (2009)
4. Chen, Y., Oliver, D.S., Zhang, D.: Efficient ensemble-based closed-loop production optimization. *SPE J.* **14**(4), 634–645 (2009)
5. Evensen, G.: *Data assimilation – the ensemble Kalman filter*, 2<sup>nd</sup> edn. Springer, Berlin (2009)
6. Fonseca, R.M., Kahrobaei, S., Van Gastel, L.J.T., Leeuwenburgh, O., Jansen, J.D.: Quantification of the impact of ensemble size on the quality of an ensemble gradient using principles of hypothesis testing. Paper 173236-MS presented at the 2015 SPE Reservoir Simulation Symposium, 22–25 February, Houston, USA (2015)

7. Howard, R.A.: Information value theory. *IEEE Transactions on Systems, Science and Cybernetics* **SSC-2**(1), 22–26 (1966)
8. Jansen, J.D., Brouwer, D.R., Nævdal, G., van Kruijsdijk, C.P.J.W.: Closed-loop reservoir management. *First Break*, January **23**, 43–48 (2005)
9. Jansen, J.D., Bosgra, O.H., van den Hof, P.M.J.: Model-based control of multiphase flow in subsurface oil reservoirs. *J. Process Control* **18**, 846–855 (2008)
10. Jansen, J.D., Douma, S.G., Brouwer, D.R., Van den Hof, P.M.J., Bosgra, O.H., Heemink, A.W.: Closed-loop reservoir management. Paper SPE 119098 presented at the SPE Reservoir Simulation Symposium, The Woodlands, USA (2009)
11. Kikani, J.: Reservoir surveillance, SPE, Richardson (2013)
12. Krymskaya, M.V., Hanea, R.G., Jansen, J.D., Heemink, A.W.: Observation sensitivity in computer-assisted history matching. In: Proceedings of the 72<sup>nd</sup> EAGE Conference & Exhibition, Barcelona (2010)
13. Le, D.H., Reynolds, A.C.: Optimal choice of a surveillance operation using information theory. *Comput. Geosci.* **18**, 505–518 (2014a)
14. Le, D.H., Reynolds, A.C.: Estimation of mutual information and conditional entropy for surveillance optimization. *SPE J.* **19**(4), 648–661 (2014b)
15. Lie, K.-A., Krogstad, S., Ligaarden, I.S., Natvig, J.R., Nilsen, H.M., Skalestad, B.: Open source MATLAB implementation of consistent discretisations on complex grids. *Comput. Geosci.* **16**(2), 297–322 (2012)
16. Nævdal, G., Brouwer, D.R., Jansen, J.D.: Waterflooding using closed-loop control. *Comput. Geosci.* **10**(1), 37–60 (2006)
17. Oliver, D.S., Reynolds, A.C., Liu, N.: Inverse theory for petroleum reservoir characterization and history matching. Cambridge University Press, Cambridge (2008)
18. Oliver, D.S., Chen, Y.: Recent progress on reservoir history matching: a review. *Comput. Geosci.* **15**(1), 185–221 (2011)
19. Sarma, P., Durlofsky, L.J., Aziz, K.: Computational techniques for closed-loop reservoir modeling with application to a realistic reservoir. *Pet. Sci. Technol.* **26**(10&11), 1120–1140 (2008)
20. Van Essen, G.M., Zandvliet, M.J., Van den Hof, P.M.J., Bosgra, O.H., Jansen, J.D.: Robust waterflooding optimization of multiple geological scenarios. *SPE J.* **14**(1), 202–210 (2009)
21. Yeten, B., Durlofsky, L.J., Aziz, K.: Optimization of nonconventional well type, location and trajectory. *SPE J.* **8**(3), 200–210 (2003)
22. Wang, C., Li, G., Reynolds, A.C.: Production optimization in closed-loop reservoir management. *SPE J.* **14**(3), 506–523 (2009)